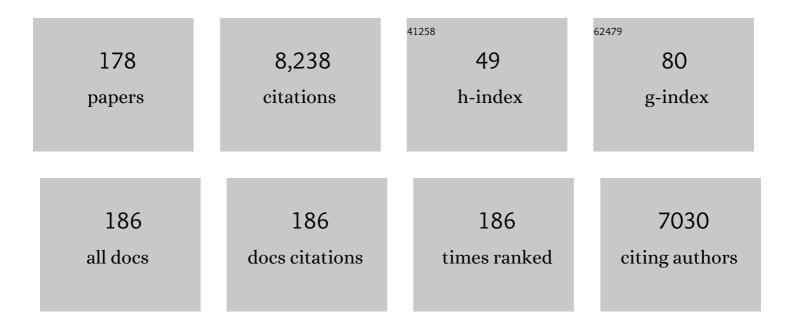
Sharon Ashbrook

List of Publications by Year in descending order

Source: https://exaly.com/author-pdf/4568499/publications.pdf Version: 2024-02-01



#	Article	IF	CITATIONS
1	First-Principles Calculation of NMR Parameters Using the Gauge Including Projector Augmented Wave Method: A Chemist's Point of View. Chemical Reviews, 2012, 112, 5733-5779.	23.0	446
2	A family of zeolites with controlled pore size prepared using a top-down method. Nature Chemistry, 2013, 5, 628-633.	6.6	355
3	Solid state170 NMR—an introduction to the background principles and applications to inorganic materials. Chemical Society Reviews, 2006, 35, 718-735.	18.7	203
4	Combining solid-state NMR spectroscopy with first-principles calculations – a guide to NMR crystallography. Chemical Communications, 2016, 52, 7186-7204.	2.2	202
5	Solid-state NMR spectroscopy. Nature Reviews Methods Primers, 2021, 1, .	11.8	196
6	The Polar Phase of NaNbO ₃ : A Combined Study by Powder Diffraction, Solid-State NMR, and First-Principles Calculations. Journal of the American Chemical Society, 2010, 132, 8732-8746.	6.6	178
7	Synthesis, characterisation and adsorption properties of microporous scandium carboxylates with rigid and flexible frameworks. Microporous and Mesoporous Materials, 2011, 142, 322-333.	2.2	170
8	Protecting group and switchable pore-discriminating adsorption properties of a hydrophilic–hydrophobic metal–organic framework. Nature Chemistry, 2011, 3, 304-310.	6.6	141
9	Structural information from quadrupolar nuclei in solid state NMR. Concepts in Magnetic Resonance Part A: Bridging Education and Research, 2006, 28A, 183-248.	0.2	136
10	Hydrolytic stability in hemilabile metal–organic frameworks. Nature Chemistry, 2018, 10, 1096-1102.	6.6	134
11	High-resolution NMR of quadrupolar nuclei in solids: the satellite-transition magic angle spinning (STMAS) experiment. Progress in Nuclear Magnetic Resonance Spectroscopy, 2004, 45, 53-108.	3.9	133
12	Early Stage Reversed Crystal Growth of Zeolite A and Its Phase Transformation to Sodalite. Journal of the American Chemical Society, 2009, 131, 17986-17992.	6.6	129
13	New Methods and Applications in Solid-State NMR Spectroscopy of Quadrupolar Nuclei. Journal of the American Chemical Society, 2014, 136, 15440-15456.	6.6	120
14	Recent advances in solid-state NMR spectroscopy of quadrupolar nuclei. Physical Chemistry Chemical Physics, 2009, 11, 6892.	1.3	114
15	Characterization of Structural Disorder in γ-Ga ₂ O ₃ . Journal of Physical Chemistry C, 2014, 118, 16188-16198.	1.5	107
16	17O and29Si NMR Parameters of MgSiO3Phases from High-Resolution Solid-State NMR Spectroscopy and First-Principles Calculations. Journal of the American Chemical Society, 2007, 129, 13213-13224.	6.6	104
17	Mixedâ€Metal MILâ€100(Sc,M) (M=Al, Cr, Fe) for Lewis Acid Catalysis and Tandem CC Bond Formation and Alcohol Oxidation. Chemistry - A European Journal, 2014, 20, 17185-17197.	1.7	104
18	Zeolites with Continuously Tuneable Porosity. Angewandte Chemie - International Edition, 2014, 53, 13210-13214.	7.2	104

#	Article	IF	CITATIONS
19	Synthesis and characterization of hybrid organic/inorganic nanotubes of the imogolite type and their behaviour towards methane adsorption. Physical Chemistry Chemical Physics, 2011, 13, 744-750.	1.3	102
20	Multiple-quantum MAS NMR of quadrupolar nuclei. Do five-, seven- and nine-quantum experiments yield higher resolution than the three-quantum experiment?. Solid State Nuclear Magnetic Resonance, 2000, 16, 203-215.	1.5	100
21	Structure and NMR assignment in calcined and as-synthesized forms of AlPO-14: a combined study by first-principles calculations and high-resolution 27Al–31P MAS NMR correlation. Physical Chemistry Chemical Physics, 2008, 10, 5754.	1.3	95
22	A novel structural form of MIL-53 observed for the scandium analogue and its response to temperature variation and CO ₂ adsorption. Dalton Transactions, 2012, 41, 3937-3941.	1.6	95
23	23Na multiple-quantum MAS NMR of the perovskites NaNbO3and NaTaO3. Physical Chemistry Chemical Physics, 2006, 8, 3423-3431.	1.3	86
24	High-Resolution ¹⁹ F MAS NMR Spectroscopy: Structural Disorder and Unusual <i>J</i> Couplings in a Fluorinated Hydroxy-Silicate. Journal of the American Chemical Society, 2010, 132, 15651-15660.	6.6	83
25	Task specific ionic liquids for the ionothermal synthesis of siliceous zeolites. Chemical Science, 2010, 1, 483.	3.7	81
26	Applications of NMR Crystallography to Problems in Biomineralization: Refinement of the Crystal Structure and ³¹ P Solid-State NMR Spectral Assignment of Octacalcium Phosphate. Journal of the American Chemical Society, 2012, 134, 12508-12515.	6.6	80
27	New Twists on the Perovskite Theme: Crystal Structures of the Elusive Phases R and S of NaNbO ₃ . Inorganic Chemistry, 2012, 51, 6876-6889.	1.9	78
28	Color and Brightness Tuning in Heteronuclear Lanthanide Terephthalate Coordination Polymers. European Journal of Inorganic Chemistry, 2013, 2013, 3464-3476.	1.0	76
29	Structural Chemistry, Monoclinic-to-Orthorhombic Phase Transition, and CO ₂ Adsorption Behavior of the Small Pore Scandium Terephthalate, Sc ₂ (O ₂ CC ₆ H ₄ CO ₂) ₃ , and Its Nitro- And Amino-Functionalized Derivatives. Inorganic Chemistry, 2011, 50, 10844-10858.	1.9	75
30	Fast room temperature lability of aluminosilicate zeolites. Nature Communications, 2019, 10, 4690.	5.8	75
31	Dynamics on the Microsecond Timescale in Microporous Aluminophosphate AlPO-14 as Evidenced by27Al MQMAS and STMAS NMR Spectroscopy. Journal of the American Chemical Society, 2006, 128, 8054-8062.	6.6	72
32	Satellite-Transition MAS NMR of Spin I=3/2, 5/2, 7/2, and 9/2 Nuclei: Sensitivity, Resolution, and Practical Implementation. Journal of Magnetic Resonance, 2002, 156, 269-281.	1.2	71
33	Recent developments in solid-state NMR spectroscopy of crystalline microporous materials. Physical Chemistry Chemical Physics, 2014, 16, 8223-8242.	1.3	69
34	Motional broadening: an important distinction between multiple-quantum and satellite-transition MAS NMR of quadrupolar nuclei. Chemical Physics Letters, 2002, 364, 634-642.	1.2	67
35	First-principles calculations of solid-state17O and29Si NMR spectra of Mg2SiO4polymorphs. Physical Chemistry Chemical Physics, 2007, 9, 1587-1598.	1.3	65
36	Control of polymorphism in NaNbO3by hydrothermal synthesis. Chemical Communications, 2009, , 68-70.	2.2	65

#	Article	IF	CITATIONS
37	Exploiting NMR spectroscopy for the study of disorder in solids. International Reviews in Physical Chemistry, 2017, 36, 39-115.	0.9	65
38	High-resolution solid-state 13C NMR spectroscopy of the paramagnetic metal–organic frameworks, STAM-1 and HKUST-1. Physical Chemistry Chemical Physics, 2013, 15, 919-929.	1.3	64
39	In situ solid-state NMR and XRD studies of the ADOR process and the unusual structure of zeolite IPC-6. Nature Chemistry, 2017, 9, 1012-1018.	6.6	63
40	Cation Disorder in Pyrochlore Ceramics: ⁸⁹ Y MAS NMR and First-Principles Calculations. Journal of Physical Chemistry C, 2009, 113, 18874-18883.	1.5	62
41	Solid-State 170 NMR Spectroscopy of Hydrous Magnesium Silicates: Evidence for Proton Dynamics. Journal of Physical Chemistry C, 2009, 113, 465-471.	1.5	61
42	2H double-quantum MAS NMR spectroscopy as a probe of dynamics on the microsecond timescale in solids. Chemical Physics Letters, 2006, 423, 276-281.	1.2	58
43	Multirate delivery of multiple therapeutic agents from metal-organic frameworks. APL Materials, 2014, 2, .	2.2	58
44	Ionothermal 17O enrichment of oxides using microlitre quantities of labelled water. Chemical Science, 2012, 3, 2293.	3.7	57
45	The pyrochlore to defect fluorite phase transition in Y2Sn2â^'xZrxO7. RSC Advances, 2013, 3, 5090.	1.7	55
46	Exploiting Periodic First-Principles Calculations in NMR Spectroscopy of Disordered Solids. Accounts of Chemical Research, 2013, 46, 1964-1974.	7.6	53
47	Multiple-quantum cross-polarization in MAS NMR of quadrupolar nuclei. Chemical Physics Letters, 1998, 288, 509-517.	1.2	52
48	Multiple-Quantum Cross-Polarization and Two-Dimensional MQMAS NMR of Quadrupolar Nuclei. Journal of Magnetic Resonance, 2000, 147, 238-249.	1.2	52
49	DFT calculations of quadrupolar solidâ€state NMR properties: Some examples in solidâ€state inorganic chemistry. Journal of Computational Chemistry, 2008, 29, 2279-2287.	1.5	52
50	93Nb NMR and DFT investigation of the polymorphs of NaNbO3. Physical Chemistry Chemical Physics, 2011, 13, 7565.	1.3	50
51	¹¹⁹ Sn MAS NMR and first-principles calculations for the investigation of disorder in stannate pyrochlores. Physical Chemistry Chemical Physics, 2011, 13, 488-497.	1.3	49
52	Synthesis and crystal chemistry of the STA-12 family of metal N,N′-piperazinebis(methylenephosphonate)s and applications of STA-12(Ni) in the separation of gases. Microporous and Mesoporous Materials, 2012, 157, 3-17.	2.2	49
53	Cost-effective ¹⁷ O enrichment and NMR spectroscopy of mixed-metal terephthalate metal–organic frameworks. Chemical Science, 2018, 9, 850-859.	3.7	49
54	Spin-locking of half-integer quadrupolar nuclei in nuclear magnetic resonance of solids: Second-order quadrupolar and resonance offset effects. Journal of Chemical Physics, 2009, 131, 194509.	1.2	48

#	Article	IF	CITATIONS
55	Facile, Room-Temperature ¹⁷ O Enrichment of Zeolite Frameworks Revealed by Solid-State NMR Spectroscopy. Journal of the American Chemical Society, 2020, 142, 900-906.	6.6	48
56	89Y Magic-Angle Spinning NMR of Y2Ti2-xSnxO7Pyrochlores. Journal of Physical Chemistry B, 2006, 110, 10358-10364.	1.2	47
57	Recent Advances in Solid-State Nuclear Magnetic Resonance Spectroscopy. Annual Review of Analytical Chemistry, 2018, 11, 485-508.	2.8	45
58	Molecular Modeling, Multinuclear NMR, and Diffraction Studies in the Templated Synthesis and Characterization of the Aluminophosphate Molecular Sieve STA-2. Journal of Physical Chemistry C, 2010, 114, 12698-12710.	1.5	44
59	A co-templating route to the synthesis of Cu SAPO STA-7, giving an active catalyst for the selective catalytic reduction of NO. Microporous and Mesoporous Materials, 2011, 146, 36-47.	2.2	44
60	Single- and multiple-quantum cross-polarization in NMR of quadrupolar nuclei in static samples. Molecular Physics, 2000, 98, 1-26.	0.8	42
61	Multinuclear Magnetic Resonance and DFT Studies of the Poly(chlorotrifluoroethylene- <i>alt</i> -ethyl vinyl ether) Copolymers. Macromolecules, 2009, 42, 5652-5659.	2.2	42
62	Synthesis, Isotopic Enrichment, and Solid-State NMR Characterization of Zeolites Derived from the Assembly, Disassembly, Organization, Reassembly Process. Journal of the American Chemical Society, 2017, 139, 5140-5148.	6.6	42
63	Exploiting the Chemical Shielding Anisotropy to Probe Structure and Disorder in Ceramics: 89Y MAS NMR and First-Principles Calculations. Journal of Physical Chemistry C, 2012, 116, 4273-4286.	1.5	41
64	Water in the Earth's mantle: a solid-state NMR study of hydrous wadsleyite. Chemical Science, 2013, 4, 1523.	3.7	41
65	Transformation of AlPO-53 to JDF-2: Reversible Dehydration of a Templated Aluminophosphate Studied by MAS NMR and Diffraction. Journal of Physical Chemistry C, 2009, 113, 10780-10789.	1.5	40
66	A Bifunctional MOF Catalyst Containing Metal–Phosphine and Lewis Acidic Active Sites. Chemistry - A European Journal, 2018, 24, 15309-15318.	1.7	40
67	170 Multiple-Quantum MAS NMR Study of High-Pressure Hydrous Magnesium Silicates. Journal of the American Chemical Society, 2001, 123, 6360-6366.	6.6	39
68	Structural Study of La _{1–<i>x</i>} Y _{<i>x</i>} ScO ₃ , Combining Neutron Diffraction, Solid-State NMR, and First-Principles DFT Calculations. Journal of Physical Chemistry C, 2013, 117, 2252-2265.	1.5	39
69	Structure and NMR assignment in AlPO4-15: A combined study by diffraction, MAS NMR and first-principles calculations. Solid State Sciences, 2009, 11, 1001-1006.	1.5	38
70	Noncovalent Interactions in Peri-Substituted Chalconium Acenaphthene and Naphthalene Salts: A Combined Experimental, Crystallographic, Computational, and Solid-State NMR Study. Inorganic Chemistry, 2012, 51, 11087-11097.	1.9	38
71	Three- and five-quantum ¹⁷ 0 MAS NMR of forsterite Mg ₂ SiO ₄ . American Mineralogist, 1999, 84, 1191-1194.	0.9	37
72	170 Multiple-Quantum MAS NMR Study of Pyroxenes. Journal of Physical Chemistry B, 2002, 106, 773-778.	1.2	37

#	Article	IF	CITATIONS
73	Relative Orientation of Quadrupole Tensors from Two-Dimensional Multiple-Quantum MAS NMR. Journal of the American Chemical Society, 2001, 123, 8135-8136.	6.6	35
74	Novel Large-Pore Aluminophosphate Molecular Sieve STA-15 Prepared Using the Tetrapropylammonium Cation As a Structure Directing Agent. Chemistry of Materials, 2010, 22, 338-346.	3.2	35
75	Synthesis of Chiral MOFâ€74 Frameworks by Postâ€5ynthetic Modification by Using an Amino Acid. Chemistry - A European Journal, 2020, 26, 13957-13965.	1.7	35
76	High-Resolution 170 NMR Spectroscopy of Wadsleyite (β-Mg2SiO4). Journal of the American Chemical Society, 2003, 125, 11824-11825.	6.6	34
77	Towards homonuclear J solid-state NMR correlation experiments for half-integer quadrupolar nuclei: experimental and simulated 11B MAS spin-echo dephasing and calculated 2JBB coupling constants for lithium diborate. Physical Chemistry Chemical Physics, 2011, 13, 5778.	1.3	34
78	Determining the Surface Structure of Silicated Alumina Catalysts via Isotopic Enrichment and Dynamic Nuclear Polarization Surface-Enhanced NMR Spectroscopy. Journal of Physical Chemistry C, 2017, 121, 22977-22984.	1.5	34
79	¹⁷ 0 NMR spectroscopy of crystalline microporous materials. Chemical Science, 2021, 12, 5016-5036.	3.7	33
80	Relative Orientation of Quadrupole Tensors from High-Resolution NMR of Powdered Solids. Journal of Physical Chemistry A, 2002, 106, 9470-9478.	1.1	32
81	Correlating fast and slow chemical shift spinning sideband patterns in solid-state NMR. Journal of Magnetic Resonance, 2005, 174, 301-309.	1.2	32
82	Calculating NMR parameters in aluminophosphates: evaluation of dispersion correction schemes. Physical Chemistry Chemical Physics, 2014, 16, 2660.	1.3	32
83	Two-dimensional satellite-transition MAS NMR of quadrupolar nuclei: shifted echoes, high-spin nuclei and resolution. Chemical Physics Letters, 2001, 345, 400-408.	1.2	31
84	Spin-locking of half-integer quadrupolar nuclei in nuclear magnetic resonance of solids: Creation and evolution of coherences. Journal of Chemical Physics, 2004, 120, 2719-2731.	1.2	31
85	Unusual Phase Behavior in the Piezoelectric Perovskite System, LixNa1–xNbO3. Inorganic Chemistry, 2013, 52, 8872-8880.	1.9	31
86	Exploiting Synthetic Conditions to Promote Structural Diversity within the Scandium(III)/Pyrimidine-4,6-dicarboxylate System. Crystal Growth and Design, 2015, 15, 2352-2363.	1.4	31
87	27Al Multiple-Quantum Magic Angle Spinning NMR Study of the Thermal Transformation between the Microporous Aluminum Methylphosphonates AlMePO-1² and AlMePO-1±. Journal of Physical Chemistry B, 1999, 103, 812-817.	1.2	30
88	Dynamics on the microsecond timescale in hydrous silicates studied by solid-state 2H NMR spectroscopy. Physical Chemistry Chemical Physics, 2010, 12, 2989.	1.3	30
89	<i>Peri</i> -Substituted Phosphorus–Tellurium Systems–An Experimental and Theoretical Investigation of the P···Te through-Space Interaction. Inorganic Chemistry, 2015, 54, 2435-2446.	1.9	30
90	Solid-state 170 nuclear magnetic resonance spectroscopy without isotopic enrichment: direct detection of bridging oxygen in radiation damaged zircon. Solid State Nuclear Magnetic Resonance, 2004, 26, 105-112.	1.5	29

#	Article	IF	CITATIONS
91	Satellite-Transition MAS NMR of Low-Î ³ Nuclei at Natural Abundance:Â Sensitivity, Practical Implementation, and Application to39K (I= 3/2) and25Mg (I= 5/2). Journal of Physical Chemistry B, 2004, 108, 13292-13299.	1.2	29
92	Ensemble-Based Modeling of the NMR Spectra of Solid Solutions: Cation Disorder in Y ₂ (Sn,Ti) ₂ O ₇ . Journal of the American Chemical Society, 2019, 141, 17838-17846.	6.6	29
93	Second-order cross-term interactions in high-resolution MAS NMR of quadrupolar nuclei. Progress in Nuclear Magnetic Resonance Spectroscopy, 2009, 55, 160-181.	3.9	28
94	Application of NMR crystallography to the determination of the mechanism of charge-balancing in organocation-templated AIPO STA-2. CrystEngComm, 2013, 15, 8668.	1.3	28
95	Probing interactions through space using spin–spin coupling. Dalton Transactions, 2014, 43, 6548-6560.	1.6	28
96	An NMR Crystallographic Investigation of the Relationships between the Crystal Structure and ²⁹ Si Isotropic Chemical Shift in Silica Zeolites. Journal of Physical Chemistry C, 2017, 121, 15198-15210.	1.5	28
97	Perspective: Current advances in solid-state NMR spectroscopy. Journal of Chemical Physics, 2018, 149, 040901.	1.2	28
98	Synthesis and Polymorphism of Mixed Aluminum–Gallium Oxides. Inorganic Chemistry, 2020, 59, 3805-3816.	1.9	28
99	Synthesis of ZIFâ€93/11 Hybrid Nanoparticles via Postâ€Synthetic Modification of ZIFâ€93 and Their Use for H ₂ /CO ₂ Separation. Chemistry - A European Journal, 2018, 24, 11211-11219.	1.7	27
100	Rotor-synchronized acquisition of quadrupolar satellite-transition NMR spectra: practical aspects and double-quantum filtration. Journal of Magnetic Resonance, 2005, 177, 44-55.	1.2	26
101	Characterisation of the (Y1â^'xLax)2Ti2O7system by powder diffraction and nuclear magnetic resonance methods. Journal of Materials Chemistry, 2006, 16, 4665-4674.	6.7	26
102	Visualization of the effect of additives on the nanostructures of individual bio-inspired calcite crystals. Chemical Science, 2019, 10, 1176-1185.	3.7	26
103	77Se Solid-State NMR of Inorganic and Organoselenium Systems: A Combined Experimental and Computational Study. Journal of Physical Chemistry C, 2011, 115, 10859-10872.	1.5	25
104	Observation of "hidden―magnesium: First-principles calculations and 25Mg solid-state NMR of enstatite. Solid State Nuclear Magnetic Resonance, 2011, 40, 91-99.	1.5	25
105	A Multinuclear NMR Study of Six Forms of AlPO-34: Structure and Motional Broadening. Journal of Physical Chemistry C, 2017, 121, 1781-1793.	1.5	25
106	High-Resolution NMR Spectroscopy of Quadrupolar Nuclei in Solids:  Satellite-Transition MAS with Self-Compensation for Magic-Angle Misset. Journal of the American Chemical Society, 2002, 124, 11602-11603.	6.6	24
107	High-resolution 170 MAS NMR spectroscopy of forsterite (Â-Mg2SiO4), wadsleyite (Â-Mg2SiO4), and ringwoodite (Â-Mg2SiO4). American Mineralogist, 2005, 90, 1861-1870.	0.9	24
108	A Multinuclear Solid-State NMR Study of Templated and Calcined Chabazite-Type GaPO-34. Journal of Physical Chemistry C, 2012, 116, 15048-15057.	1.5	24

#	Article	IF	CITATIONS
109	Unusual Intermolecular "Through-Space― <i>J</i> Couplings in P–Se Heterocycles. Journal of the American Chemical Society, 2015, 137, 6172-6175.	6.6	24
110	Octaselenocyclododecane. Angewandte Chemie - International Edition, 2011, 50, 4123-4126.	7.2	23
111	Investigating Relationships between the Crystal Structure and ³¹ P Isotropic Chemical Shifts in Calcined Aluminophosphates. Journal of Physical Chemistry C, 2014, 118, 23285-23296.	1.5	23
112	Exploring the self-assembly and energy transfer of dynamic supramolecular iridium-porphyrin systems. Dalton Transactions, 2016, 45, 17195-17205.	1.6	23
113	Modulatorâ€Controlled Synthesis of Microporous STAâ€26, an Interpenetrated 8,3â€Connected Zirconium MOF with the <i>theâ€i</i> Topology, and its Reversible Lattice Shift. Chemistry - A European Journal, 2018, 24, 6115-6126.	1.7	23
114	New insights into phase distribution, phase composition and disorder in Y ₂ (Zr,Sn) ₂ O ₇ ceramics from NMR spectroscopy. Physical Chemistry Chemical Physics, 2015, 17, 9049-9059.	1.3	22
115	Paramagnetic NMR of Phenolic Oxime Copper Complexes: A Joint Experimental and Density Functional Study. Chemistry - A European Journal, 2016, 22, 15328-15339.	1.7	22
116	STA-27, a porous Lewis acidic scandium MOF with an unexpected topology type prepared with 2,3,5,6-tetrakis(4-carboxyphenyl)pyrazine. Journal of Materials Chemistry A, 2019, 7, 5685-5701.	5.2	22
117	A procedure for identifying possible products in the assembly–disassembly–organization–reassembly (ADOR) synthesis of zeolites. Nature Protocols, 2019, 14, 781-794.	5.5	22
118	A multiple-quantum 23Na MAS NMR study of amorphous sodium gallium silicate zeolite precursors. Journal of Materials Chemistry, 2002, 12, 1469-1474.	6.7	21
119	Detecting solid-state reactivity in 10-hydroxy-10,9-boroxophenanthrene using NMR spectroscopy. Tetrahedron, 2010, 66, 6238-6250.	1.0	21
120	Investigation of zeolitic imidazolate frameworks using 13 C and 15 N solid-state NMR spectroscopy. Solid State Nuclear Magnetic Resonance, 2017, 87, 54-64.	1.5	21
121	Pressure-induced chemistry for the 2D to 3D transformation of zeolites. Journal of Materials Chemistry A, 2018, 6, 5255-5259.	5.2	21
122	Kinetics and Mechanism of the Hydrolysis and Rearrangement Processes within the Assembly–Disassembly–Organization–Reassembly Synthesis of Zeolites. Journal of the American Chemical Society, 2019, 141, 4453-4459.	6.6	21
123	Novel two-dimensional NMR methods that combine single-quantum cross-polarization and multiple-quantum MAS of quadrupolar nuclei. Chemical Physics Letters, 2001, 340, 500-508.	1.2	20
124	Efficient Amplitude-Modulated Pulses for Triple- to Single-Quantum Coherence Conversion in MQMAS NMR. Journal of Physical Chemistry A, 2014, 118, 6018-6025.	1.1	19
125	Conformational Dependence of Throughâ€Space Tellurium–Tellurium Spin–Spin Coupling in <i>Peri</i> â€Substituted Bis(Tellurides). Chemistry - A European Journal, 2015, 21, 3613-3627.	1.7	19
126	Hunting for hydrogen: random structure searching and prediction of NMR parameters of hydrous wadsleyite. Physical Chemistry Chemical Physics, 2016, 18, 10173-10181.	1.3	19

#	Article	IF	CITATIONS
127	Solidâ€State NMR Spectroscopy Proves the Presence of Pentaâ€coordinated Sc Sites in MILâ€100(Sc). Chemistry - A European Journal, 2017, 23, 9525-9534.	1.7	19
128	Sterically Restricted Tin Phosphines, Stabilized by Weak Intramolecular Donor–Acceptor Interactions. Organometallics, 2014, 33, 2424-2433.	1.1	18
129	[1,2,5]Selenadiazolo[3,4â€ <i>b</i>]pyrazines: Synthesis from 3,4â€Diaminoâ€1,2,5â€selenaÂdiazole and Genera of Persistent Radical Anions. European Journal of Organic Chemistry, 2015, 2015, 5585-5593.	ition 1.2	18
130	Selective Oxidation and Functionalization of 6-Diphenylphosphinoacenaphthyl-5-tellurenyl Species 6-Ph ₂ P-Ace-5-TeX (X = Mes, Cl, O ₃ SCF ₃). Various Types of P–E···Te(II,IV) Bonding Situations (E = O, S, Se). Organometallics, 2017, 36, 1566-1579.	1.1	18
131	Nuclear Overhauser Effect (NOE) Enhancement of 11B NMR Spectra of Borane Adducts in the Solid State. Journal of the American Chemical Society, 2006, 128, 6782-6783.	6.6	17
132	Solid-state NMR measurements and DFT calculations of the magnetic shielding tensors of protons of water trapped in barium chlorate monohydrate. RSC Advances, 2014, 4, 56248-56258.	1.7	17
133	Ionothermal synthesis and characterization of CoAPO-34 molecular sieve. Microporous and Mesoporous Materials, 2017, 239, 336-341.	2.2	17
134	NMR chemical shifts of urea loaded copper benzoate. A joint solid-state NMR and DFT study. Solid State Nuclear Magnetic Resonance, 2019, 101, 31-37.	1.5	17
135	SCAM-STMAS: satellite-transition MAS NMR of quadrupolar nuclei with self-compensation for magic-angle misset. Journal of Magnetic Resonance, 2003, 162, 402-416.	1.2	16
136	Following the unusual breathing behaviour of ¹⁷ O-enriched mixed-metal (Al,Ga)-MIL-53 using NMR crystallography. Physical Chemistry Chemical Physics, 2020, 22, 14514-14526.	1.3	16
137	Phase Composition and Disorder in La ₂ (Sn,Ti) ₂ O ₇ Ceramics: New Insights from NMR Crystallography. Journal of Physical Chemistry C, 2016, 120, 20288-20296.	1.5	15
138	Investigating Unusual Homonuclear Intermolecular "Through-Space―J Couplings in Organochalcogen Systems. Inorganic Chemistry, 2016, 55, 10881-10887.	1.9	15
139	Formation Mechanism and Porosity Development in Porous Boron Nitride. Journal of Physical Chemistry C, 2021, 125, 27429-27439.	1.5	15
140	An NMR crystallographic approach to monitoring cation substitution in the aluminophosphate STA-2. Solid State Nuclear Magnetic Resonance, 2015, 65, 64-74.	1.5	14
141	STARTMAS: A MAS-based method for acquiring isotropic NMR spectra of spin I=3/2 nuclei in real time. Chemical Physics Letters, 2006, 431, 390-396.	1.2	13
142	A Modular Approach for the Synthesis of Nanometer-Sized Polynitroxide Multi-Spin Systems. Journal of Organic Chemistry, 2014, 79, 8313-8323.	1.7	13
143	¹⁷ O solid-state NMR spectroscopy of A ₂ B ₂ O ₇ oxides: quantitative isotopic enrichment and spectral acquisition?. RSC Advances, 2018, 8, 7089-7101.	1.7	13
144	A Picture of Disorder in Hydrous Wadsleyite—Under the Combined Microscope of Solid-State NMR Spectroscopy and Ab Initio Random Structure Searching. Journal of the American Chemical Society, 2019, 141, 3024-3036.	6.6	13

#	Article	IF	CITATIONS
145	Phosphorus–Bismuth <i>Peri</i> -Substituted Acenaphthenes: A Synthetic, Structural, and Computational Study. Inorganic Chemistry, 2020, 59, 5616-5625.	1.9	13
146	Effects of Extraframework Species on the Structure-Based Prediction of ³¹ P Isotropic Chemical Shifts of Aluminophosphates. Journal of Physical Chemistry C, 2017, 121, 28065-28076.	1.5	12
147	Mechanochemically assisted hydrolysis in the ADOR process. Chemical Science, 2020, 11, 7060-7069.	3.7	12
148	Solid-State NMR of High-Pressure Silicates in the Earth's Mantle. Annual Reports on NMR Spectroscopy, 2013, 79, 241-332.	0.7	11
149	Calculation and experimental measurement of paramagnetic NMR parameters of phenolic oximate Cu(<scp>ii</scp>) complexes. Chemical Communications, 2017, 53, 10512-10515.	2.2	11
150	13C pNMR of "crumple zone―Cu(II) isophthalate metal-organic frameworks. Solid State Nuclear Magnetic Resonance, 2019, 101, 44-50.	1.5	11
151	Single-step synthesis and interface tuning of core–shell metal–organic framework nanoparticles. Chemical Science, 2021, 12, 4494-4502.	3.7	11
152	Investigating FAM-N pulses for signal enhancement in MQMAS NMR of quadrupolar nuclei. Solid State Nuclear Magnetic Resonance, 2017, 84, 89-102.	1.5	9
153	Nuclear Magnetic Resonance Spectroscopy as a Dynamical Structural Probe of Hydrogen under High Pressure. Physical Review Letters, 2019, 122, 135501.	2.9	9
154	Application of NMR Crystallography to Highly Disordered Templated Materials: Extensive Local Structural Disorder in the Gallophosphate GaPO-34A. Inorganic Chemistry, 2020, 59, 11616-11626.	1.9	9
155	Investigation of the hydrothermal crystallisation of the perovskite solid solution NaCe1â^'La Ti2O6 and its defect chemistry. Journal of Solid State Chemistry, 2013, 207, 117-125.	1.4	8
156	Alkaline-Earth Rhodium Hydroxides: Synthesis, Structures, and Thermal Decomposition to Complex Oxides. Inorganic Chemistry, 2018, 57, 11217-11224.	1.9	8
157	Phase Distribution, Composition, and Disorder in Y ₂ (Hf,Sn) ₂ O ₇ Ceramics: Insights from Solid-State NMR Spectroscopy and First-Principles Calculations. Journal of Physical Chemistry C, 2020, 124, 17073-17084.	1.5	7
158	Porous zinc and cobalt 2-nitroimidazolate frameworks with six-membered ring windows and a layered cobalt 2-nitroimidazolate polymorph. CrystEngComm, 2017, 19, 1377-1388.	1.3	6
159	Is the <scp>³¹P</scp> chemical shift anisotropy of aluminophosphates a useful parameter for <scp>NMR</scp> crystallography?. Magnetic Resonance in Chemistry, 2019, 57, 176-190.	1.1	6
160	Solid-state host–guest influences on a BODIPY dye hosted within a crystalline sponge. New Journal of Chemistry, 2020, 44, 14108-14115.	1.4	6
161	The ambient hydration of the aluminophosphate JDF-2 to AlPO-53(A): insights from NMR crystallography. Acta Crystallographica Section C, Structural Chemistry, 2017, 73, 191-201.	0.2	6
162	An expanded MIL-53-type coordination polymer with a reactive pendant ligand. CrystEngComm, 2018, 20, 4355-4358.	1.3	5

#	Article	IF	CITATIONS
163	Thermal Dehydrofluorination of GaPO-34 Revealed by NMR Crystallography. Journal of Physical Chemistry C, 2021, 125, 2537-2545.	1.5	5
164	Post-synthetic modification of zinc metal-organic frameworks through palladium-catalysed carbon–carbon bond formation. Journal of Organometallic Chemistry, 2015, 792, 134-138.	0.8	4
165	A gel aging effect in the synthesis of open-framework gallium phosphates: structure solution and solid-state NMR of a large-pore, open-framework material. Dalton Transactions, 2017, 46, 16895-16904.	1.6	4
166	Polymorphism, Weak Interactions and Phase Transitions in Chalcogen–Phosphorus Heterocycles. Chemistry - A European Journal, 2018, 24, 11067-11081.	1.7	4
167	Siteâ€Specific Iron Substitution in STAâ€28, a Large Pore Aluminophosphate Zeotype Prepared by Using 1,10â€Phenanthrolines as Frameworkâ€Bound Templates. Angewandte Chemie - International Edition, 2020, 59, 15186-15190.	7.2	4
168	SERS of Trititanate Nanotubes: Selective Enhancement of Catechol Compounds. ChemistrySelect, 2018, 3, 8338-8343.	0.7	3
169	Sensitivity improvement in 5QMAS NMR experiments using FAM-N pulses. Solid State Nuclear Magnetic Resonance, 2019, 100, 1-10.	1.5	3
170	Rationalization of solid-state NMR multi-pulse decoupling strategies: Coupling of spin l = ½ and half-integer quadrupolar nuclei. Journal of Magnetic Resonance, 2019, 303, 48-56.	1.2	3
171	Siteâ€Specific Iron Substitution in STAâ€28, a Large Pore Aluminophosphate Zeotype Prepared by Using 1,10â€Phenanthrolines as Frameworkâ€Bound Templates. Angewandte Chemie, 2020, 132, 15298-15302.	1.6	2
172	Origin of the temperature dependence of ¹³ C pNMR shifts for copper paddlewheel MOFs. Chemical Science, 2022, 13, 2674-2685.	3.7	2
173	NMR spectroscopy of paramagnetic solids. Solid State Nuclear Magnetic Resonance, 2019, 104, 101625.	1.5	1
174	Recent advances in solidâ€state nuclear magnetic resonance spectroscopy of quadrupolar nuclei. Magnetic Resonance in Chemistry, 2021, 59, 851-852.	1.1	1
175	Reply to Comment on "27Al Multiple-Quantum Magic Angle Spinning NMR Study of the Thermal Transformation between the Microporous Aluminum Methylphosphonates AlMePO-β and AlMePO-α― Journal of Physical Chemistry B, 2000, 104, 9767-9767.	1.2	0
176	High-Resolution NMR of Quadrupolar Nuclei in Solids: The Satellite-Transition Magic Angle Spinning (STMAS) Experiment. ChemInform, 2004, 35, no.	0.1	0
177	Inside Cover: Conformational Dependence of Throughâ€Space Tellurium–Tellurium Spin–Spin Coupling in <i>Peri</i> â€Substituted Bis(Tellurides) (Chem. Eur. J. 9/2015). Chemistry - A European Journal, 2015, 21, 3506-3506.	1.7	0
178	Exploring cation disorder in mixedâ€metal pyrochlore ceramics using ¹⁷ 0 NMR spectroscopy and firstâ€principles calculations. Magnetic Resonance in Chemistry, 2021, 59, 961-974.	1.1	0